

Dipolar-Induced Resonance for Ultracold Bosons in a Quasi-1D Optical Lattice

N. Bartolo^{1,2}, D.J. Papoular¹, L. Barbiero^{3,4}, C. Menotti¹, A. Recati¹

¹*INO-CNR BEC Center and Dipartimento di Fisica, Università di Trento, 38123 Povo, Italy*

²*Laboratoire Charles Coulomb, CNRS, Université Montpellier 2, France*

³*Dipartimento di Fisica e Astronomia "Galileo Galilei", Università di Padova, Italy*

⁴*Laboratoire de Physique Théorique, CNRS, Université de Toulouse, France*

We study the role of the dipolar interaction, correctly accounting for the Dipolar-Induced Resonance (DIR), in a quasi-one-dimensional system of ultracold bosons. We first show how the DIR affects the lowest-energy states of two particles in a harmonic trap. Then, we consider a deep optical lattice loaded with ultracold dipolar bosons. We describe this many-body system using an atom-dimer extended Bose-Hubbard model. We analyze the impact of the DIR on the phase diagram at $T = 0$ by exact diagonalization of a small-sized system. In particular, the resonance strongly modifies the range of parameters for which a mass density wave should occur.

Introduction. The recent experimental developments in the field of ultracold dipolar gases have opened up fascinating prospects for the study of systems exhibiting Dipole-Dipole Interaction (DDI) [1, 2]. Bose-Einstein Condensates (BECs) of magnetic atoms have been realized using Chromium [3], Erbium [4], and Dysprosium [5]. However, the magnetic moments carried by single atoms are small ($\lesssim 10 \mu_B$, where μ_B is the Bohr magneton), and therefore the effects of the DDI observed with these systems have remained perturbative up to now [6]. The recent realization of the ultracold heteronuclear molecules RbK [7] and NaK [8], which both carry electric dipole moments of the order of one Debye, offer a promising route towards stronger DDI effects, but quantum degeneracy still remains to be achieved with these systems. Rydberg atoms boast much larger dipole moments and will provide an alternative way to explore the DDI, but yield challenging experimental problems associated with time and length scales [9].

The DDI is both anisotropic and long-ranged, and dipolar gases thus allow for the quantum simulation of more general Hamiltonians than the ones accessible with non-dipolar neutral particles, whose interaction is described by the standard s -wave interaction [10]. Furthermore, the trapping techniques available for ultracold atoms makes it possible to control the effective dimensionality. The use of a lower dimensionality stabilizes the system with respect to two-body and many-body instabilities caused by the attractive part of the three-dimensional DDI. This has prompted detailed studies of dipolar systems in 2D and quasi-2D [11–15], bilayer [16–18], and quasi-1D [19–21] geometries.

Experiments involving dipolar bosons in optical lattices have recently been performed both with atomic BECs [22] and non-condensed dipolar molecules [23]. The simplest theoretical description of such dipolar systems in a lattice is provided by an Extended Bose-Hubbard Model (EBHM) accounting for nearest-neighbour interactions [1]. The 1D EBHM has already been explored theoretically for generic values of the model parameters, revealing the occurrence, beyond

the standard Mott-Insulator (MI) and superfluid (SF) phases, of a Mass Density Wave (MDW) phase [21, 24] and a Haldane Insulator phase [25, 26].

In this Letter, we study ultracold bosonic dipoles in an optical lattice, in the quasi-1D tight-binding regime [27, 28]. In order to obtain accurate predictions corresponding to our specific system, our model should include the effect of the Dipolar Induced Resonance (DIR) [29, 30]. The DIR is a low-energy scattering resonance which occurs when the dipole strength is varied. Accounting for it requires going beyond the single-band EBHM [31]. We develop an atom-dimer EBHM, which is the simplest possible lattice model reproducing the DIR.

The scattering and bound-state properties of the DDI have been studied numerically for free-space models [32] as well as systems trapped in 3D and 2D optical lattices [33]. In our quasi-1D geometry, we describe the interaction using an effective potential obtained by averaging the transverse degrees of freedom into the corresponding harmonic oscillator ground state [19, 20]:

$$V_{1D}(x) = \left(g_{1D} - \frac{\hbar^2}{m} \frac{2r^*}{3l_\perp^2} \right) \delta(x) + \frac{\hbar^2}{m} \frac{r^*}{l_\perp^3} \left[\sqrt{\frac{\pi}{8}} e^{\frac{1}{2} \frac{x^2}{l_\perp^2}} \left(\frac{x^2}{l_\perp^2} + 1 \right) \text{Erfc} \left(\frac{|x|}{\sqrt{2}l_\perp} \right) - \frac{|x|}{2l_\perp} \right], \quad (1)$$

where $r^* = mD^2/\hbar^2$ is the dipolar length, with D being the dipolar strength. The range of this potential is determined by the oscillator length $l_\perp = (\hbar/m\omega_\perp)^{1/2}$ in the strongly-confined directions y and z . The term $g_{1D} = 2\hbar^2 a_{3D}/ml_\perp^2$ is the strength of the standard s -wave contact interaction for a 3D scattering length a_{3D} [34], which can be manipulated using a Feshbach resonance [35]. It competes with the DDI to determine the stability and the phase of the system [36]. For simplicity, we assume $g_{1D} = 0$ unless otherwise specified. Note that, under this assumption, the potential defined by Eq. (1) still contains a contact term proportional to r^* .

Two-body physics. The basic building block of our many-body lattice Hamiltonian (see Eq. (4) below) is provided by the solution of the two-body problem in a

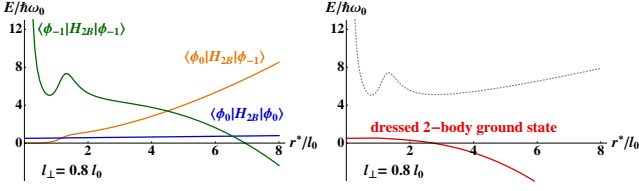


FIG. 1. (Color online). Left: matrix elements of the two-state Hamiltonian $H_{2\text{state}}$ describing two bosonic dipoles in a harmonic trap, as a function of the dipolar length r^* . Right: corresponding ground-state (red) and excited-state (dashed grey) energies.

single lattice site. Hence, we solve for the ground state of two dipolar bosons in a single quasi-1D harmonic well, with the axial trapping frequency ω_0 and the corresponding oscillator length $l_0 = (\hbar/m\omega_0)^{1/2}$. The quasi-1D hypothesis requires the ratio l_\perp/l_0 to be small. In this two-body problem, the center-of-mass and relative motions are decoupled. The relative motion is governed by the following Hamiltonian:

$$H_{2B} = p^2/2m_r + m_r\omega_0^2 x^2/2 + V_{1D}(x), \quad (2)$$

where x is the interparticle distance, p is its conjugate momentum, and $m_r = m/2$ is the reduced mass.

Unlike in the case of the contact interaction solved in [37], the Hamiltonian H_{2B} cannot be diagonalized analytically. Therefore, we seek its ground state numerically, by considering the restriction of H_{2B} onto a subspace spanned by a finite number of suitably chosen basis states $\{|\phi_n\rangle\}$. Depending on the value of r^* , the effective interaction V_{1D} supports either no bound state or a single one. The bound state is present for large enough values of r^* , and its entrance coincides with the occurrence of the DIR. The ‘bare’ bound state supported by the attractive contact part of $V_{1D}(x)$ plays a key role. The corresponding wavefunction is $\psi_{BS}(x) = \sqrt{\kappa} \exp(-\kappa|x|)$, where $\kappa = r^*/(3l_\perp^2)$, and its cusp at $x = 0$ cannot be reproduced by projecting $|\psi_{BS}\rangle$ onto a subspace spanned by any finite number of harmonic oscillator eigenstates which are all smooth at $x = 0$. This implies that the DIR physics can only be captured if a wavefunction which has a cusp at $x = 0$ is included in the basis $\{|\phi_n\rangle\}$. The smallest such basis contains two elements, and we choose it to be $\{|\phi_0\rangle, |\phi_{-1}\rangle\}$, where $|\phi_0\rangle$ is the ground state of the 1D harmonic oscillator with frequency ω_0 , and $|\phi_{-1}\rangle \propto |\psi_{BS}\rangle - \langle\phi_0|\psi_{BS}\rangle|\phi_0\rangle$ is a linear combination of $|\psi_{BS}\rangle$ and $|\phi_0\rangle$ chosen such that the basis is orthonormal. Hence, for a given value of the dipolar length r^* , we replace H_{2B} by the following two-state Hamiltonian:

$$H_{2\text{state}} = \begin{pmatrix} \langle\phi_0|H_{2B}|\phi_0\rangle & \langle\phi_0|H_{2B}|\phi_{-1}\rangle \\ \langle\phi_{-1}|H_{2B}|\phi_0\rangle & \langle\phi_{-1}|H_{2B}|\phi_{-1}\rangle \end{pmatrix}. \quad (3)$$

The diagonalization of $H_{2\text{state}}$ (see Fig. 1) yields approximations of the ground-state energy $E_{2B}(r^*)$ and wavefunction $|\Psi_{2B}(r^*)\rangle$. The energy E_{2B} thus obtained is

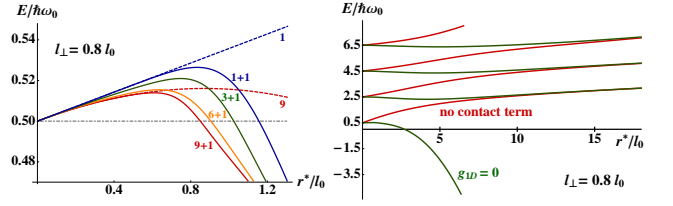


FIG. 2. (Color online). Left: Ground-state energy $E_{2B}(r^*)$ of the Hamiltonian H_{2B} , for $g_{1D} = 0$ and $l_\perp/l_0 = 0.8$, including 1 (blue), 3 (green), 6 (orange), and 9 (red) harmonic oscillator states, without (dashed lines) and with (solid lines) the ‘bare’ bound state $|\phi_{-1}\rangle$ in the projection basis. Right: the four lowest eigenvalues of H_{2B} as a function of r^* , for $g_{1D} = 0$ (green) and choosing $g_{1D} = 2\hbar^2 r^*/(3ml_\perp^2)$ to cancel the contact term (red), calculated including four harmonic oscillator states and the ‘bare’ bound state $|\phi_{-1}\rangle$ in the basis.

plotted as a function of r^* in Fig. 1(right) for $l_\perp/l_0 = 0.8$. Including a greater number of harmonic oscillator states in the basis allows for the calculation of higher-energy states (see Fig. 2 (right)). However, as shown on Fig. 2(left), it does not affect the qualitative behavior of the ground-state energy $E_{2B}(r^*)$ as long as the bound state $|\phi_{-1}\rangle$ is also included in the basis.

The non-monotonic behaviour of $E_{2B}(r^*)$ (Fig. 1 (right)) is a signature of the DIR. In particular, the ground state energy goes below $\hbar\omega_0/2$ for $r^* > r_{\text{crit}}^*$, where $r_{\text{crit}}^*/l_0 = 1.16$ for $l_\perp/l_0 = 0.8$. Correspondingly, the ground-state wavefunction exhibits a cusp, which signals a strong contamination from the ‘bare’ bound state $|\phi_{-1}\rangle$. However, the main point for the many-body treatment described below is that the population of the bound state is very small: the overlap $|\langle\phi_{-1}|\Psi_{2B}\rangle|^2$ remains smaller than 0.05 for $r^* \lesssim r_{\text{crit}}^*$. This overlap only becomes substantial if the states $|\phi_0\rangle$ and $|\phi_{-1}\rangle$ have comparable energies, i.e. for $r^*/l_0 \gtrsim 6.5$ (see Fig. 1(left)). The contamination of the wavefunction occurring much earlier than the crossing of the bare energy levels can be traced back to the shape-resonance nature of the DIR [29], and distinguishes it from Feshbach resonances, which usually occur near the crossing of the bare levels [35]. More details regarding the scattering properties associated with V_{1D} and the DIR will be given elsewhere [38].

The right-hand plot of Fig. 2 shows the energies of the four lowest-energy states of H_{2B} as a function of r^* in two different situations: (i) the s -wave interaction term $g_{1D} = 0$ (green curves) and (ii) the term g_{1D} is non-zero and chosen such as to cancel the contact term in Eq. (1) completely [20]. The r^* -dependence of the energy levels we predict in these two situations is completely different. This will allow for an observation of the DIR using the spectroscopic techniques presented, e.g., in [39].

Many-body physics. We now consider N dipolar particles loaded into a deep quasi-1D optical lattice with unity filling factor. We describe this system using a Bose-

Hubbard model [10, 40] extended to include nearest-neighbour interactions. We focus on the regime $r^* \lesssim r_{\text{crit}}^*$, so that the DIR affects the two-body properties even though the number of dimers present in the system is extremely small. In order to properly account for the resonance, we start from the two-state description introduced above for the two-body problem (Eq. (3)). In the presence of the coupling between the N different sites of the lattice, each of the two states $|\phi_0\rangle$ and $|\phi_{-1}\rangle$ yields a band and, hence, we introduce an atom-dimer EBHM which reads:

$$H_{\text{AD}} = \sum_i [\varepsilon_a n_i + \frac{U}{2} n_i(n_i - 1) - J_a(a_i^\dagger a_{i+1} + \text{hc}) + V n_i n_{i+1} + \varepsilon_d m_i - J_d(b_i^\dagger b_{i+1} + \text{hc}) + \Omega(b_i^\dagger a_i a_i + \text{hc})] . \quad (4)$$

In Eq. (4), a_i and b_i are the annihilation operators in the site i for atoms and dimers, respectively, and $n_i = a_i^\dagger a_i$ and $m_i = b_i^\dagger b_i$ are the corresponding number operators. The atomic tunnelling coefficient J_a is taken from [41]. We extract the on-site energy for single atoms and dimers, ε_a and ε_d , the atomic on-site interaction energy U , and the atom-dimer conversion rate Ω , from the matrix elements of H_{2state} (Eq. (3)). The atomic nearest-neighbour interaction coefficient V is expressed in terms of the effective interaction V_{1D} (Eq. (1)) and the Gaussian approximation to the Wannier function $w_i(x)$ localized on site i . The nearly-vanishing population of the dimer band for $r^* \lesssim r_{\text{crit}}^*$ allows for a very crude description of the dimer dynamics: we neglect atom-dimer and dimer-dimer interaction, and we take $J_d = J_a/10$ in our numerics. The scaling for J_d follows from the assumption that the polarizability of a molecule is twice that of a single atom [41]. In any case, in the regime we consider, the exact value of J_d does not affect our numerical results.

We focus on the tight-binding regime and we introduce the harmonic oscillator length l_0 characterizing the bottom of each lattice well. Like for the two-body problem described above, we consider a fixed value of l_\perp/l_0 , which determines the aspect ratio of the system. The ground state of the system then depends on two adimensional parameters: r^*/l_0 and V/U . The choice of the parameter r^*/l_0 allows for a direct comparison with the two-body physics illustrated in Figs. 1 and 2. In the case of the DDI with $g_{1D} = 0$, the ratio V/U does not depend on r^* . It strongly decays with the lattice depth $s = V_{\text{lat}}/E_R$, where V_{lat} is the intensity of the optical lattice and E_R is the recoil energy. The validity of the harmonic approximation used to determine the single-site parameters requires s to be large enough and thus imposes an upper bound on V/U .

For given values of r^*/l_0 and V/U , we numerically calculate the ground state of the EBHM described by Eq. (4) by exact diagonalization of a 6-atom, 6-well system. In Fig. 3, we plot the phase diagram of the system as a function of these two variables. The observable is the single-particle off-diagonal density matrix element

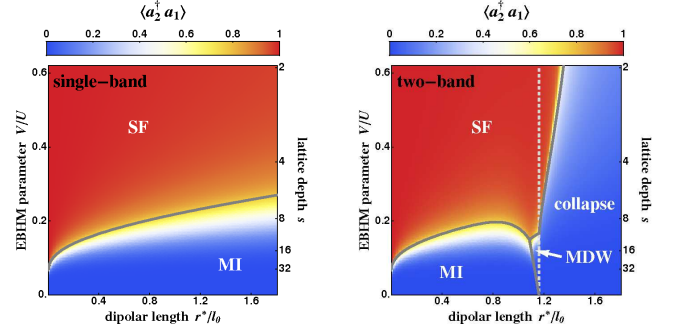


FIG. 3. (Color online). Many-body phase diagrams obtained using the single-band ($\Omega = 0$, left) and atom-dimer ($\Omega > 0$, right) EBHMs, performing exact diagonalization on a six-atom, six-well system with $l_\perp/l_0 = 0.8$. The effective on-site interaction $U_{\text{eff}} < 0$ on the right of the vertical dashed line.

$\rho_1 = \langle a_2^\dagger a_1 \rangle$, and it distinguishes the superfluid phase ($\rho_1 \neq 0$) from the insulating phases ($\rho_1 = 0$). The different insulating phases can subsequently be told apart by looking at the projection of the ground-state wavefunction onto all accessible configurations. Figure 3 compares the phase diagram obtained using the single-band EBHM (i.e. taking $\Omega = 0$ in Eq. (4)) with the one obtained using the atom-dimer EBHM ($\Omega > 0$) for the same range of parameters which satisfy the constraints mentioned above. Up to a change of units to $(U/J, V/J)$, and in the parameter range for which our model is valid, the single-band phase diagram is equivalent to the one presented in [24], and it exhibits two phases: superfluid (SF) and Mott-insulator (MI). The two-band phase diagram is qualitatively different. In particular, the MI phase region stops at $r^* = r_{\text{crit}}^*$, and two additional phases appear, which are schematically represented in Fig. 4(right): a (twice degenerate) Mass Density Wave (MDW) phase with a spatial period which is twice the lattice period, and a ‘collapse’ phase (which is N -fold degenerate) where all atoms sit in the same well. In our small-sized system, the MI-MDW and MDW-collapse transitions appear sharp, in accordance with the first-order character expected to accompany a change in discrete symmetry. On the contrary, the transitions between the SF phase and each insulating phase are smooth, which is compatible with the predicted Berezinskii-Kosterlitz-Thouless-like behaviour expected in 1D [24].

The phase diagram shown in Figs. 3(right) and 4(left) can be interpreted in terms of an effective single-band EBHM, with the on-site interaction coefficient reproducing the two-body ground-state energy:

$$H_{\text{eff}} = \sum_i [\varepsilon_a n_i + \frac{U_{\text{eff}}}{2} n_i(n_i - 1) - J_a(a_i^\dagger a_{i+1} + \text{hc}) + V n_i n_{i+1}] , \quad (5)$$

where $U_{\text{eff}}(r^*) = E_{2B}(r^*) - \hbar\omega_0/2$. In the parameter range explored on Figs. 3 and 4(left), the phase diagram obtained by exact diagonalization of H_{eff} is very similar to the two-band phase diagram. This is due to the de-

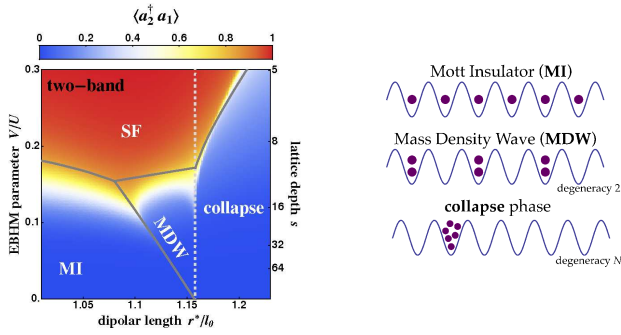


FIG. 4. (Color online). Left: Zoom-in on the central part of the atom-dimer phase diagram (Fig. 3 (right), $l_\perp/l_0 = 0.8$) showing the transitions between the SF, MI, MDW, and collapse phases. Right: cartoon representations of the three insulating phases for six atoms in six wells.

tuning $\Delta = \epsilon_d - U - 2\epsilon_a$ between the atom and dimer bands being much larger than Ω , J_a and V [42]. The effective single-band model (Eq. (5)) allows for a direct comparison between the phase diagram we present and those calculated in terms of the usual EBHM parameters U/J and V/J . In particular, we find a Haldane-like phase near the upper left corner of our MDW domain, which is compatible with the Haldane phase domain reported in [26]. A systematic investigation of the Haldane phase domain is beyond the scope of the present Letter and will be carried out on larger-sized systems using DMRG [38].

We also use this effective model to derive quasi-analytical approximations of the phase boundaries for any number N of particles and sites. For two given contiguous phases, we calculate the energy of each phase in terms of J , U_{eff} , V , and N , using the form of the wavefunction valid deep within each phase. Equating these two energies, we obtain the grey lines shown for $N = 6$ on Figs. 3 and 4. We now consider more specifically the boundary between the SF and the collapse phases, given by $E_{\text{SF}} - E_{\text{collapse}} \approx N(V - 2J) - N^2 U_{\text{eff}}/2 = 0$. The tunnelling term scales linearly with N , whereas the on-site interaction term scales with N^2 . Therefore, for small N , the superfluid phase survives in a region where $U_{\text{eff}} < 0$, but the collapse phase is energetically favored for large N . This instability favoring the collapse phase corresponds to the implosion of a Bose-Einstein condensate with a negative scattering length when its size is increased [43].

Conclusion. We have studied the effect of the DDI in quasi-1D geometries both from the two-body and the many-body perspectives. From the two-body point of view, we have shown how the DIR affects the dependence of the energies of the first few excited states of the system on the dipolar strength D . Concerning the many-body physics, we have pointed out that the DIR makes it possible to reach the MDW phase for lower values of V/U , and that the system collapses into a single lattice site for larger values of D , for which the effective on-site

interaction U_{eff} becomes negative. The predicted phases may be experimentally identified using in-situ imaging techniques as well as the recent advances allowing for the detection of non-local order [44].

We studied the effect of the two-body DIR on the many-body physics using the minimal EBHM. The DIR could also have a strong effect on systems described by generalized EBHMs such as the one studied in, e.g., [15]. It would be interesting to extend this work to 2D geometries, where the anisotropy of the dipolar interaction is expected to play a role. We believe our analysis would also be relevant for the understanding of the fermionic 1D EBHM with repulsive interactions, where the relevant phases are the Spin Density Wave (SDW), the Charge Density Wave (CDW), and the Bond Order Wave (BOW) [45–48].

We acknowledge stimulating discussions with M. Baranov, G. Ferrari, L.P. Pitaevskii, G.V. Shlyapnikov, S. Stringari, and W. Zwerger. L.B. acknowledges the hospitality of the BEC Center, Trento, during the initial stage of the project. This work has been supported by ERC through the QGBE grant.

-
- [1] T. Lahaye, C. Menotti, L. Santos, M. Lewenstein, and T. Pfau, Rep. Prog. Phys. **72**, 126401 (2009)
 - [2] M. A. Baranov, M. Dalmonte, G. Pupillo, and P. Zoller, Chem. Rev. **112**, 5012 (2012)
 - [3] A. Griesmaier, J. Werner, S. Hensler, J. Stuhler, and T. Pfau, Phys. Rev. Lett. **94**, 160401 (2005)
 - [4] K. Aikawa, A. Frisch, M. Mark, S. Baier, A. Rietzler, R. Grimm, and F. Ferlaino, Phys. Rev. Lett. **108**, 210401 (2012)
 - [5] M. Lu, N. Q. Burdick, S. H. Youn, and B. Lev, Phys. Rev. Lett. **107**, 190401 (2011)
 - [6] J. Stuhler, A. Griesmaier, T. Koch, M. Fattori, T. Pfau, S. Giovanazzi, P. Pedri, and L. Santos, Phys. Rev. Lett. **95**, 150406 (2005)
 - [7] K.-K. Ni, S. Ospelkaus, M. G. H. de Miranda, A. Pe'er, B. Neyenhuis, J. J. Zirbel, S. Kotochigova, P. S. Julienne, D. S. Jin, and J. Ye, Science **322**, 231 (2008)
 - [8] C.-H. Wu, J. W. Park, P. Ahmadi, S. Will, and M. W. Zwierlein, Phys. Rev. Lett. **109**, 085301 (2012)
 - [9] M. Saffman, T. G. Walker, and K. Molmer, Rev. Mod. Phys. **82**, 2313 (2010)
 - [10] I. Bloch, J. Dalibard, and S. Nascimbène, Nat. Phys. **8**, 267 (2012)
 - [11] N. Matveeva and S. Giorgini, Phys. Rev. Lett. **109**, 200401 (2012)
 - [12] Z.-K. Lu and G. V. Shlyapnikov, Phys. Rev. A **85**, 023614 (2012)
 - [13] M. Babadi and E. Demler, Phys. Rev. B **84**, 235124 (2011)
 - [14] M. Babadi, B. Skinner, M. M. Fogler, and E. Demler (2012), arXiv:1212.1493
 - [15] T. Sowinski, O. Dutta, P. Hauke, L. Tagliacozzo, and M. Lewenstein, Phys. Rev. Lett. **108**, 115301 (2012)
 - [16] A. Pikovski, M. Klawunn, G. V. Shlyapnikov, and L. San-

- tos, Phys. Rev. Lett. **105**, 215302 (2010)
- [17] M. Klawunn and A. Recati(2011), arXiv:1110.2336
 - [18] C.-K. Chan, C. Wu, W.-C. Lee, and S. D. Sarma, Phys. Rev. A **81**, 023602 (2010)
 - [19] S. Sinha and L. Santos, Phys. Rev. Lett. **99**, 140406 (2007)
 - [20] F. Deuretzbacher, J. C. Cremon, and S. M. Reimann, Phys. Rev. A **81**, 063616 (2010)
 - [21] A. Maluckov, G. Gligoric, L. Hadzievski, B. A. Malomed, and T. Pfau, Phys. Rev. Lett. **108**, 140402 (2012)
 - [22] B. Pasquiou, G. Bismut, E. Maréchal, P. Pedri, L. Vernac, O. Gorceix, and B. Laburthe-Tolra, Phys. Rev. Lett. **106**, 015301 (2011)
 - [23] A. Chotia, B. Neyenhuis, S. A. Moses, B. Yan, J. P. Covey, M. Foss-Feig, A. M. Rey, D. S. Jin, and J. Ye, Phys. Rev. Lett. **108**, 080405 (2012)
 - [24] R. V. Pai and R. Pandit, Phys. Rev. B **71**, 104508 (2005)
 - [25] E. G. Dalla Torre, E. Berg, and E. Altman, Phys. Rev. Lett. **97**, 260401 (2006)
 - [26] D. Rossini and R. Fazio, New J. Phys. **14**, 065012 (2012)
 - [27] C. Trefzger, C. Menotti, B. Capogrosso-Sansone, and M. Lewenstein, J. Phys. B **44**, 193001 (2011)
 - [28] I. Bloch, J. Dalibard, and W. Zwerger, Rev. Mod. Phys. **80**, 885 (2008)
 - [29] M. Marinescu and L. You, Phys. Rev. Lett. **81**, 4596 (1998)
 - [30] Z. Shi, R. Qui, and H. Zhai, Phys. Rev. A **85**, 020702 (2012)
 - [31] H. P. Büchler, Phys. Rev. Lett. **104**, 090402 (2010)
 - [32] K. Kanjilal and D. Blume, Phys. Rev. A **78**, 040703 (2008)
 - [33] T. M. Hanna, E. Tiesinga, W. F. Mitchell, and P. S. Julienne, Phys. Rev. A **85**, 022703 (2012)
 - [34] D. S. Petrov, G. V. Shlyapnikov, and J. T. M. Walraven, Phys. Rev. Lett. **85**, 3745 (2000)
 - [35] C. Chin, R. Grimm, P. Julienne, and E. Tiesinga, Rev. Mod. Phys. **82**, 1225 (2010)
 - [36] T. Koch, T. Lahaye, J. Metz, B. Fröhlich, A. Griesmaier, and T. Pfau, Nat. Phys. **4**, 218 (2008)
 - [37] T. Busch, B. Englert, K. Rzazewski, and M. Wilkens, Found. Phys. **28**, 549 (1998)
 - [38] Same authors, In preparation
 - [39] J. Hecker-Denschlag, J. E. Simsarian, H. Häffner, C. McKenzie, A. Browaeys, D. Cho, K. Helmerson, S. L. Rolston, and W. D. Phillips, J. Phys. B **35**, 3095 (2002)
 - [40] M. P. A. Fisher, P. B. Weichman, G. Grinstein, and D. S. Fisher, Phys. Rev. B **40**, 546 (1989)
 - [41] F. Gerbier, A. Widera, S. Fölling, O. Mandel, T. Gericke, and I. Bloch, Phys. Rev. A **72**, 053606 (2005), typo corrected.
 - [42] The two-band results and the effective one-band results are expected to differ for small detunings Δ . In this case, the dimer population is non-negligible and the crude approximation of the dimer dynamics in Eq. (4) is no longer applicable.
 - [43] E. A. Donley, N. R. Claussen, S. L. Cornish, J. L. Roberts, E. A. Cornell, and C. E. Wieman, Nature **412**, 295 (2001)
 - [44] M. Endres, M. Cheneau, T. Fukuhara, C. Weitenberg, P. Schauss, C. Gross, L. Mazza, M. C. Banuls, L. Pollet, I. Bloch, and S. Kuhr, Science **334**, 200 (2011)
 - [45] S. Ejima and S. Nishimoto, Phys. Rev. Lett. **99**, 216403 (2007)
 - [46] M. Nakamura, Phys. Rev. B **61**, 16377 (2000)
 - [47] S. G. Bhongale, L. Mathey, S.-W. Tsai, C. W. Clark, and E. Zhao, Phys. Rev. Lett. **108**, 145301 (2012)
 - [48] L. Barbiero, M. Dalmonte, M. D. Dio, and A. Recati, In preparation